



# Ultra-Long Crystalline Red Phosphorus Nanowires from Amorphous Red Phosphorus Thin Films

Joshua B. Smith, Daniel Hagaman, David DiGuseppi, Reinhard Schweitzer-Stenner, and Hai-Feng Ji\*

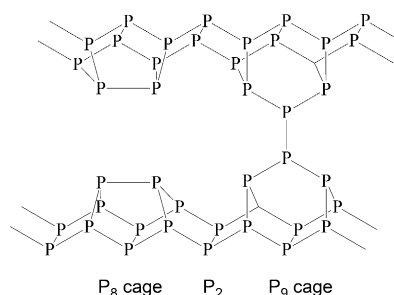
**Abstract:** Heating red phosphorus in sealed ampoules in the presence of a  $\text{Sn/SnI}_4$  catalyst mixture has provided bulk black phosphorus at much lower pressures than those required for allotropic conversion by anvil cells. Herein we report the growth of ultra-long 1D red phosphorus nanowires ( $> 1 \text{ mm}$ ) selectively onto a wafer substrate from red phosphorus powder and a thin film of red phosphorus in the presence of a  $\text{Sn/SnI}_4$  catalyst. Raman spectra and X-ray diffraction characterization suggested the formation of crystalline red phosphorus nanowires. FET devices constructed with the red phosphorus nanowires displayed a typical  $I$ - $V$  curve similar to that of black phosphorus and a similar mobility reaching  $300 \text{ cm}^2 \text{ V}^{-1} \text{ s}^{-1}$  with an  $I_{\text{on}}/I_{\text{off}}$  ratio approaching  $10^2$ . A significant response to infrared light was observed from the FET device.

The discovery of carbon nanotubes and the isolation of graphene from bulk graphite has led to extensive research in the field of 1D and 2D materials and their applications. Applications have been investigated in areas including field-effect transistors, photodetectors, and solar cells. These discoveries have intrigued researchers to investigate the formation and applications of 1D and 2D materials from another elemental allotrope, phosphorus. Phosphorus exists as three different allotropes; white, red (violet belongs to one type of red), and black. White phosphorus is made of  $\text{P}_4$  molecules. Red phosphorus has been found to exist as a number of crystalline forms all of which exhibit a reddish color.<sup>[1]</sup> Type I was found to form under the normal thermal conversion of white phosphorus from  $250^\circ\text{C}$  to  $280^\circ\text{C}$  and products obtained were amorphous.<sup>[2]</sup> Types II and III were found to have very diffuse X-ray patterns and it was noted that a potential mixture could have existed, as there was a short range of temperatures in which type III can be formed.<sup>[2]</sup> Type IV form of red phosphorus<sup>[2]</sup> was further investigated recently and was termed “fibrous red phosphorus”.<sup>[3]</sup> The type V form of red phosphorus was observed as heating continued past  $550^\circ\text{C}$ .<sup>[1,3-5]</sup> The type V form was also termed Hittorf’s phosphorus or violet phosphorus.<sup>[1,6,7]</sup> Both

fibrous red phosphorus (type IV) and violet phosphorus (type V) are predominantly made up of a phosphorus chain containing  $\text{P}_8$  and  $\text{P}_9$  cages that link together to form tube-like structures.<sup>[4]</sup> These tubes are oriented parallel to each other between layers in type IV,<sup>[4]</sup> and perpendicular to one another between layers in type V.<sup>[4,8]</sup> Black phosphorus (BP) is composed of corrugated, continuous six-member rings forming sheets of covalently bonded phosphorus atoms in the orthorhombic form.<sup>[1,9-11]</sup> It was not until recently that a low-temperature/pressure method to obtain black phosphorus was discovered. Lange et al. found that black phosphorus could be grown from red phosphorus at  $873 \text{ K}$  in a sealed ampoule in the presence of gold, tin, and tin(IV) iodide.<sup>[12]</sup> The method was then optimized to eliminate the need for additional side products and it was found that removal of the gold from the system still allowed for low-pressure/temperature growth of black phosphorus.<sup>[13]</sup>

The intrinsic band gap of the orthorhombic crystalline structure of black phosphorus, especially the 2D black phosphorus thin films, provides a variety of potential applications without the need for doping of the material, which attracted attention in the last two years.<sup>[14,15]</sup> While the attention paid to 2D black phosphorus thin films has been rapidly growing in the last two years, there are only a few reports on the formation and properties of 1D phosphorus wires.

In a study by Ruck et al. in 2005,<sup>[3]</sup> 1D red phosphorus nanowires were synthesized by heating red phosphorus in an evacuated ampoule around  $590^\circ\text{C}$  for several days. The structure was determined to exist as an arrangement of double tubes formed from the  $\text{P}_8$  and  $\text{P}_9$  cages as shown in Scheme 1. The work by Eckstein et al. revealed that a single-phase of “urchin-like” 1D fibrous phosphorus microwires can be synthesized in the presence of  $\text{CuCl}_2$  as a mineralizing agent.<sup>[16]</sup> The fibers that were grown with this method



**Scheme 1.** Arrangement of the double tubes along the fiber axis in 1D fibrous phosphorus.

[\*] J. B. Smith, D. Hagaman, D. DiGuseppi, Prof. R. Schweitzer-Stenner, Prof. H.-F. Ji  
Department of Chemistry  
Drexel University  
Philadelphia, PA 19104 (USA)  
E-mail: hj56@drexel.edu

Supporting information and the ORCID identification number(s) for the author(s) of this article can be found under <http://dx.doi.org/10.1002/anie.201605516>.

typically ranged from 25–50  $\mu\text{m}$  in diameter. Shen et al.<sup>[17]</sup> showed the selective growth of 1D nanowires on raw silicon during an elongated heating process of red phosphorus in a sealed ampoule. The length ranges from 20 to 30  $\mu\text{m}$  with diameters of 400–600 nm, depending on the amount of red phosphorus starting materials in the sealed ampoule. Another investigation on the 1D red phosphorus form was carried out by Winchester et al. in 2009.<sup>[18]</sup> They grew wires starting from white phosphorus in the presence of a bismuth doped silicon wafer and the ampoules were heated in the temperature range of 300–460 °C. Winchester et al. found that these reaction conditions formed the type II form of red phosphorus, which were also in the form of short rod or fiber-like structures. The phosphorus nanorods were found to exist from 3 to 5  $\mu\text{m}$  in length and 300–400 nm in diameter.

Recently, we developed a method to growth larger 2D BP thin films with a modified BP growth method.<sup>[19]</sup> Following this work, attempts at conversion of these thin films of red phosphorus directly into black phosphorus, all within a sealed ampoule, led to a unique discovery of ultra-long and uniform 1D phosphorus nanowires. Herein, we report the formation conditions and the characterization of these nanowires. We also investigated the applicability of these nanowires as a field effect transistor (FET) device and an infrared light responsive device.

The synthesis of ultra-long nanowires involves two steps. First, we prepared a thin red phosphorus film on a  $\text{SiO}_2$ /silicon wafer (300 nm oxide thickness, Montco Silicon, the wafer was cut to a desired size of roughly 0.75 cm  $\times$  0.25 cm) in a quartz tube according to a procedure we recently reported.<sup>[19]</sup> Briefly, 0.5 mg of red phosphorus powder was placed at the end of a quartz tube and a wafer substrate was placed at the opening of the tube furnace. The tube was sealed in vacuum and then heated in a tube furnace to 600 °C for 30 min. When the tube was cooled, the red phosphorus thin film appeared as a green film on the surface of the wafer substrate. In our previous study we demonstrated that a green colored red phosphorus thin film corresponds to a thickness of around 40 nm and a blue color corresponds to thinner films with a thickness of under 10 nm, which were confirmed by AFM measurements.<sup>[19]</sup>

In the subsequent step, purified red phosphorus powder (110 mg) along with  $\text{SnI}_4$  (15 mg) and Sn powder (30 mg) were placed into an ampoule with the bottom end sealed. The phosphorus film coated silicon wafer plate, approximately 6 cm in length, was also placed into the ampoule. The ampoule was then capped with a rubber septum and evacuated/backfilled ( $5\times$ ) with approximately 1 atm of argon. The ampoules were then flame sealed in 1 atm argon and allowed to cool. Once cooled, the ampoules were placed into a furnace and heated to 630 °C. This temperature was maintained for 1 h and then slowly decreased (10 °C/15 min) until the temperature reached 500 °C. The ampoules remained at 500 °C for one additional hour and then the furnace was turned off. Once the temperature reached 400 °C, the ampoules were removed and placed on the bench top until cooled to room temperature. The images in Figure 1 show typical appearances of silicon wafer plates before and after the heating process (not the same plate).



**Figure 1.** Left: Image of sealed ampoule, containing red phosphorus thin film on an  $\text{SiO}_2$ /Si silicon-wafer plate, prior to reaction. Right: Image of phosphorus nanowire network on the silicon-wafer plate.

As the sealed ampoule was broken open, several regions of the silicon plate had a fuzzy appearance. When observed with bright field microscopy, a large network of wires was noticed (Figure 2a). Wires were visible on the plate and were darker in color with a fuzzy appearance. A majority of the samples were black, while some regions of the plate appeared

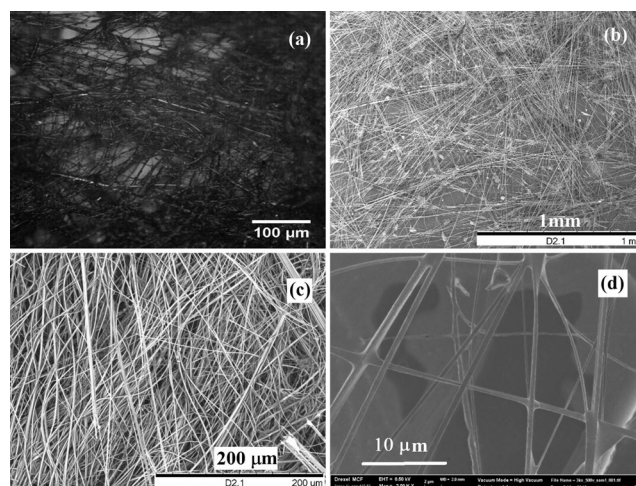


**Figure 2.** Images of ultra-long phosphorus nanowires. a) Bright-field image of phosphorus microwire network. b) Nanowires grown on substrate show varying lengths exceeding 1 mm. c) A dense network of phosphorus nanowires, and d) an enlarged section of the nanowire network.

red. When viewed with the optical microscope, the red color was determined to be result of residual red phosphorus powder that deposited over the top of the wires. Lengths of the wires were observed to exceed 1 mm with diameters of 300–800 nm. Samples were immediately transferred to a vacuum desiccator until further analysis was carried out. If not, droplets began to appear on the wires from water absorption and formation of phosphoric acid after several minutes under ambient conditions (Figure S1 supporting information). Air sensitivity was only observed with a few samples, primarily the smaller sized nanowires, and some wires survived without any observable decomposition for several days out of a dessicator. There are two possible explanations: the first is a size effect as smaller nanowires are more reactive because of larger surface area; and the second is the possibility that the sample is not pure, but a mixture of allotropes, with the majority of them being type IV (and V, see the discussion below), which is relatively more stable than other red allotropes. An improvement in yield or purification of the type IV nanowires is under investigation and will be

reported in the future. SEM imaging of the nanowires showed a large number of uniform nanowires in all different directions (Figure 2b). Figure 2c,d shows a dense network of wires and an enlarged section of the nanowire network.

It should be noted that an “urchin-like” structures seemed to be selectively formed on the inside of the glass ampoule and the ultra-long nanowire formation was primarily selectively formed on the silicon-wafer substrate (Figure S2 supporting information). The “urchin-like” structures were observed and discussed by Shen et al.<sup>[17]</sup> These structures appeared more like rods rather than needles or wires.

It is also noteworthy that the growth of ultra-long phosphorus nanowires may be carried out when red phosphorus powder was used to convert into nanowires directly on a plain silicon-wafer plate in the ampoule. However, more uniform and much larger quantity of ultra-long nanowires can be obtained when a red phosphorus thin film on the silicon wafer is used, suggesting the thin red phosphorus film prepared in the first step provided favorable nucleation sites for the growth of ultra-long nanowires.

To identify the allotropic form of these ultra-long nanowires, Raman spectroscopy, powder X-ray diffraction (XRD), and transmission electron microscopy (TEM) of the wires were studied.

Raman spectra were obtained on these samples (Figure 3). The primary Raman signals appear at 353 and 368  $\text{cm}^{-1}$ , whereas less-intense bands appear at 393, 436, 452, and 471  $\text{cm}^{-1}$ . The Raman spectra suggest a good mix of the  $\text{P}_8$  and  $\text{P}_9$  cages. According to Fasol et al. the 368  $\text{cm}^{-1}$  peak belongs to the stretching vibrations of the  $\text{P}_8$  cages, and the

353  $\text{cm}^{-1}$  peak is the stretching vibrations of the  $\text{P}_9$  cages.<sup>[20]</sup> Winchester et al.'s work<sup>[18]</sup> had an excellent summary of Raman spectra of white, black, and type II and type IV red phosphorus. The Raman peaks from nanowires agree the most with the literature studies on type IV fibrous red phosphorus, although we cannot rule out the type V Hittorf's phosphorus, since the Raman spectra of type IV and type V are quite similar (Figure 3b).<sup>[18]</sup>

Powder X-ray diffraction (XRD) experiments were conducted and the result is shown in Figure 4. The d-spacing value of the nanowires shows peaks at 5.85, 4.97, 3.18, 2.91, 2.04, 1.90, 1.67, 1.63, and 1.61 Å. Again, based on Winchester

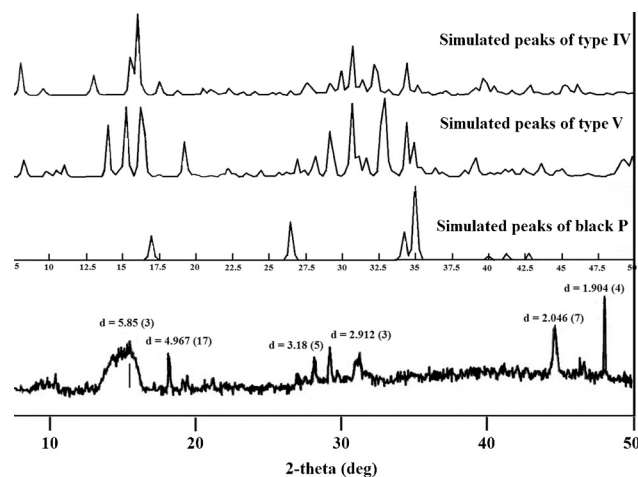


**Figure 4.** XRD of phosphorus nanowires and those simulated from CIF files of black phosphorus, type IV, and type V red phosphorus by using Reciprograph.

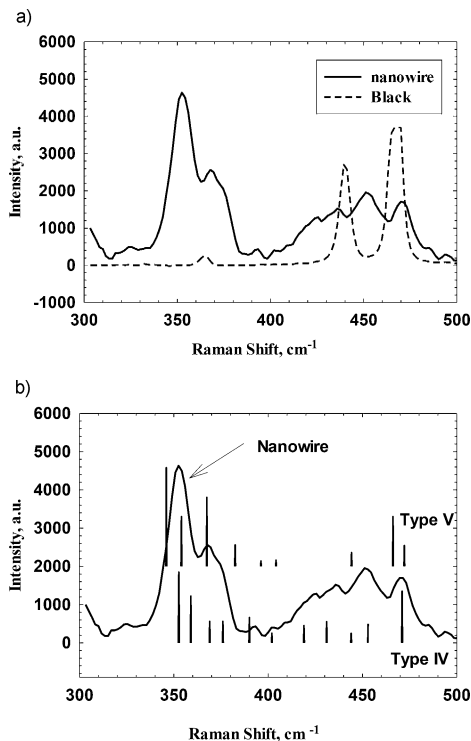


**Figure 3.** Raman spectra of phosphorus nanowires with a) black phosphorus and b) reported peaks with intensity and location from literature for type IV<sup>[19]</sup> and V.<sup>[18]</sup>

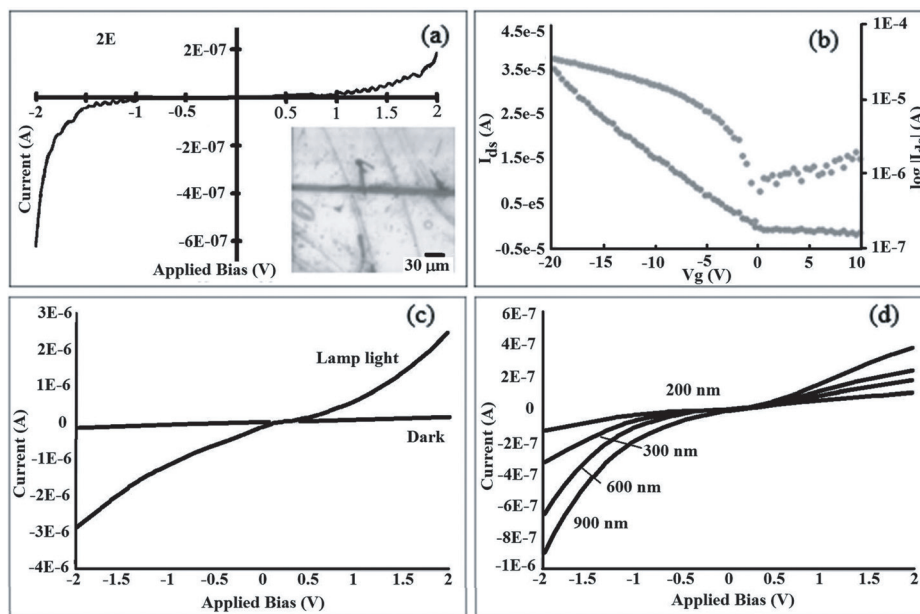
et al.'s summary,<sup>[18]</sup> these values do not match with those of the black phosphorus and type II red phosphorus, and were in the best agreement with the data on type IV fibrous red phosphorus,<sup>[2,3,17]</sup> which is consistent with the observation from the Raman spectra. Again, we cannot rule out type V red phosphorus. The comparison of XRD of the nanowires with simulated XRDs of black phosphorus, types IV and V red phosphorus is shown in Figure 4.

Figure 5 shows the TEM and SAED patterns of a single 400-nm-diameter nanowire. The wires appeared a cylindrical shape, and showed a clear crystallinity, as observed from the SAED pattern. Several d-spacing values were 2.64, 2.85, 3.02 Å. Those peaks from the diffraction pattern were not found for black phosphorus, but can only be found for types IV and V red phosphorus.<sup>[2]</sup> It is noteworthy that they are not likely type V violet phosphorus as the SAED pattern is significantly different from TEM SAED pattern of type V violet phosphorus (see Supporting Information). Besides, we could obtain high-resolution TEM images from the violet phosphorus sample, but not from nanowires because the nanowires decompose under high voltage when collecting high-resolution TEM images. Based on these results, the nanowires are more likely to be type IV phosphorus although it is possible some violet phosphorus was present in the sample as well. Temperature seems to play a major role. In our experiment, 600–630 °C was used to



prepare the type IV red phosphorus nanowires. For making violet phosphorus, temperatures of 650–750 °C seems a good range (see Supporting Information). For preparing black phosphorus, temperature higher than 950 °C is needed as seen from our previous observation.<sup>[19]</sup> However, factors such as reaction time, cooling time and pressure also contribute to the yield and uniformity of the morphologies, which will be further investigated in the future.

Previous work carried out on type IV fibrous phosphorus formation found that the material was capable of generating holes and electrons through a photocatalytic study,<sup>[17]</sup> indicating type IV red phosphorus may have useful applications similar to black phosphorus. In our work, electrical characterization of these wires brought about an *I*–*V* curve that resembles that of black phosphorus and a semiconductor material with a slightly higher resistance (Figure 6a). FET measurements were performed on this same sample and the *I*–*V* curves show this phosphorus wire structure functioning as a transistor (Figure 6b). This device has a fairly low  $I_{\text{on}}/I_{\text{off}}$  ratio of approximately  $10^2$ , however, the mobility can be estimated from these samples and this was found to be  $308 \text{ cm}^2 \text{ V}^{-1} \text{ s}$ . This shows a high mobility for fibrous red phosphorus and a value similar to



**Figure 6.** a) *I*–*V* curve of phosphorus wire. Inset of bright-field image. b) Transfer plots of phosphorus wire showing gate dependence with p-type characteristics. c), d) *I*–*V* curves with of phosphorus wires functioning as a photodetector. c) Response for complete dark conditions and full light from Xe lamp and d) response from 200 nm to 900 nm.

black phosphorus samples. This is the first reported mobility values of fibrous phosphorus in the literature. Brief investigations into the potential use for these phosphorus wires as optoelectronic devices were carried out using the assembled device shown above. The effects of various wavelengths on the *I*–*V* curves were studied within the wavelength range from 200–900 nm. Figure 6c shows the *I*–*V* curve responses from dark conditions to full light conditions. The full light was provided by a 150 W Xe bulb from a Hitachi 7000 fluorimeter. Figure 6d shows this same device with an increasing current as the light is varied from 200–900 nm. This shows the potential infrared photodetector application of these long phosphorus nanowires.

The heating of amorphous red phosphorus powder and a thin film of red phosphorus film on a silicon wafer in a sealed ampoule resulted in the discovery of a mm-long, uniform, and dense phosphorus nanowire network. Raman analysis and XRD suggest the nanowires are more likely type IV, fibrous red phosphorus than type V red phosphorus. FET devices were constructed with the nanowires, which is the first time this has been investigated with the fibrous form. A typical *I*–*V* curve similar to that of black phosphorus was apparent. The nanowire has a mobility around the  $300 \text{ cm}^2 \text{ V}^{-1} \text{ s}$  range with an  $I_{\text{on}}/I_{\text{off}}$  ratio approaching  $10^2$ . A significant response to infrared light was observable with the *I*–*V* curves. The fibrous form of red phosphorus may provide another potential source for applications in such fields as batteries, sensors, and optoelectronic devices.

## Acknowledgements

This work was supported by SARI-Drexel seed grant.

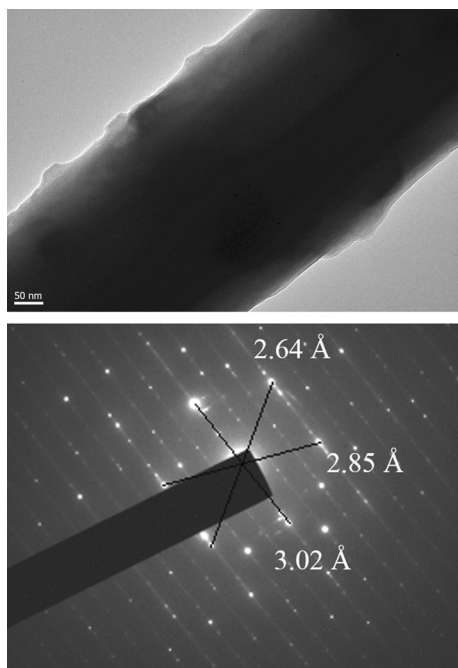


**Figure 5.** Top: TEM image of a phosphorus nanowire and bottom: its respective SAED patterns. Several d-spacing values are labeled.

**Keywords:** black phosphorus · conductive materials · nanowires · red phosphorus · transistors

**How to cite:** *Angew. Chem. Int. Ed.* **2016**, 55, 11829–11833  
*Angew. Chem.* **2016**, 128, 12008–12012

- 
- [1] D. E. C. Corbridge, *Phosphorus: Chemistry, Biochemistry and Technology*, 6th ed., CRC Press, **2013**.
- [2] W. L. Roth, T. W. DeWitt, A. J. Smith, *J. Am. Chem. Soc.* **1947**, 69, 2881–2885.
- [3] M. Ruck, D. Hoppe, B. Wahl, P. Simon, Y. Wang, G. Seifert, *Angew. Chem. Int. Ed.* **2005**, 44, 7616–7619; *Angew. Chem.* **2005**, 117, 7788–7792.
- [4] H. Thurn, H. Krebs, *Angew. Chem. Int. Ed. Engl.* **1966**, 5, 1047–1048; *Angew. Chem.* **1966**, 78, 1101–1102.
- [5] A. V. Frost, *J. Russ. Phys. Chem. Soc.* **1930**, 62, 2235–2241.
- [6] F. Bachhuber, J. von Appen, R. Dronskowski, P. Schmidt, T. Nilges, A. Pfizner, R. Wehrich, *Angew. Chem. Int. Ed.* **2014**, 53, 11629–11633; *Angew. Chem.* **2014**, 126, 11813–11817.
- [7] M. Hittor, *Philos. Mag.* **1865**, 31, 311.
- [8] H.-S. Tsai, C.-C. Lai, C.-H. Hsiao, H. Medina, T.-Y. Su, H. Ouyang, T.-H. Chen, J.-H. Liang, Y.-L. Chueh, *ACS Appl. Mater. Interfaces* **2015**, 7, 13723–13727.
- [9] Y. Maruyama, S. Suzuki, K. Kobayashi, S. Tanuma, *Phys. B + C* **1981**, 105, 99–102.
- [10] R. Hultgren, N. S. Gingrich, B. E. Warren, *J. Chem. Phys.* **1935**, 3, 351–355.
- [11] L. Cartz, S. R. Srinivasa, R. J. Riedner, J. D. Jorgensen, T. G. Worlton, *J. Chem. Phys.* **1979**, 71, 1718–1721.
- [12] S. Lange, P. Schmidt, T. Nilges, *Inorg. Chem.* **2007**, 46, 4028–4035.
- [13] M. Köpf, N. Eckstein, D. Pfister, C. Grotz, I. Krüger, M. Greiwe, T. Hansen, H. Kohlmann, T. Nilges, *J. Cryst. Growth* **2014**, 405, 6–10.
- [14] H. Liu, A. Neal, Z. Zhu, Z. Luo, X. Xu, *ACS Nano* **2014**, 4, 4033–4041.
- [15] J. Wu, N. Mao, L. Xie, H. Xu, J. Zhang, *Angew. Chem. Int. Ed.* **2015**, 54, 2366–2369; *Angew. Chem.* **2015**, 127, 2396–2399.
- [16] N. Eckstein, A. Hohmann, R. Wehrich, T. Nilges, P. Schmidt, *Z. Anorg. Allg. Chem.* **2013**, 639, 2741–2743.
- [17] Z. Shen, Z. Hu, W. Wang, S.-F. Lee, D. K. L. Chan, Y. Li, T. Gu, J. C. Yu, *Nanoscale* **2014**, 6, 14163–14167.
- [18] R. L. Winchester, M. Whitby, M. S. P. Shaffer, *Angew. Chem. Int. Ed.* **2009**, 48, 3616–3621; *Angew. Chem.* **2009**, 121, 3670–3675.
- [19] J. B. Smith, D. Hagaman, H.-F. Ji, *Nanotechnology* **2016**, 27, 215602.
- [20] G. Fasol, M. Cardona, W. Hönle, H. G. von Schnering, *Solid State Commun.* **1984**, 52, 307–310.
- 

Received: June 7, 2016

Revised: July 23, 2016

Published online: August 24, 2016